Turk J Phy
24 (2000) , 701 – 708.

Synthesis and Characteristics of Nickel Manganite by Lithiation

S. V. SALVI, M. R. PARAB
Department of Physics The Institute of Science
15 / M. C. Road Mumbai - 400 032-INDIA

Received 02.02.1998

Abstract

Spinel nickel manganite has been synthesized using ceramic technique, from ($2MnO_2$+NiO) mixture reduced using $LiAlH_4$. Powder X-ray diffractometry (XRD) indicates the formation of cubic spinel (a=8.33 A°), while IR absorption spectral features are rather broad, though similar to those of spinel. The d.c. electrical conductivity of the ceramic is much smaller than that reported for $NiMn_2O_4$. Even though the band gap remains the same, when the sintering temperature is increased from 950°C to 1100 °C, all other changes are insignificant except that the porosity and particle size nearly halve. The characteristics of the system are discussed in terms of 'lithiation'.

1. Introduction

Interest in $NiMn_2O_4$ is due to its high conductivity which may have use in negative temperature coefficient thermistors [1-5]. $NiMn_2O_4$ is basically an inverse spinel [6] having cation distribution Mn_{γ}^{2+} $Ni_{1-\gamma}^{2+}$ ($Ni_{\gamma}^{2+}Mn_{2(1-\gamma)}^{3+}$ Mn_{γ}^{4+})O_4 [7]. As a slow-cooled ceramic, γ is approximately 0.93. However, at about 400 °C, there is a sudden change in cation distribution. For a specimen quenched from 940 °C, γ is equal to 0.74. For the present study, ceramics of $NiMn_2O_4$ have been prepared at around 1200 °C [8-9]. In the present communication, the spinel is prepared using MnO_2. Further, the sample is deliberately reduced and the spinel is obtained at 950°C for oxides. The structural and electrical properties of these ceramics are reproduced here.

2. Experimental

NaOH is added to the pink solution of $MnCl_2.4H_2O$ and a white precipitate is obtained. By heating the precipitate at 850 °C, fine powder of MnO_2 is obtained. Fine powders of MnO_2 and A.R. grade NiO are mixed thoroughly in 2:1 molecular weight

proportion. The mixture is sintered at 900 °C for 24 hours for homogenization (sample 1/S1). As such MnO_2 reportedly reduces to Mn_2O_3 at 530°C and to Mn_3O_4 at 950°C [10]. However, the XRD analysis of S1 does not reveal a spinel phase. Assuming no reduction of MnO_2, and to stabilise the overall valency of manganese to +3, $LiAlH_4$ is added in ratio according to the following formula:

$$2MnO_2 + NiO + 0.5\ LiAlH_4.$$

The mixture is crushed into a fine powder and sintered at 950°C for 12 hours (sample 2/S2). The procedure is repeated at 1100 °C (sample 3/S3).

The XRD patterns of the fine powders of all the samples are obtained on a microprocessor based JDX-X-ray diffractometer fabricated by JEOL. The infrared spectroscopic studies had been carried out on a PERKIN ELMER 1600 series FTIR spectrophotometer. The d.c. resistivity as a function of temperature is measured by two probe method using silver paste contacts.

3. Results and Discussion

The XRD pattern of sample 1 (Figure 1a) does not reveal a definite pattern. However, the reflections corresponding to reactants are also absent. Thus, it indicates the commencement of reaction and is characterised by the amorphous nature of the sample. The XRD pattern corresponding to sample 2 (Figure 1b)) is well developed. Its structure is a FCC spinel having lattice constant a = 8.325 Å. The pattern of sample 3 (Figure 1c) also corresponds to a crystalline material and a FCC spinel (a = 8.330 Å).

The observed interplanar distances and relative intensities along with calculated interplanar distances, Miller indices and particle sizes are shown in Tables 1 & 2 for samples 2 & 3, respectively. The lattice constants, the observed densities, porosities [11], the average particle sizes [12] and homogeneities [13] for samples 2 & 3 are compared in Table 3. From Table 3, it is seen that the porosity and particle size are larger for sample 2. The large porosity may be due to the reaction with the reducing agent ($LiAlH_4$). The particle size at 1100 °C is nearly half of that at 950°C. This may be due to increased random distribution of cations at higher sintering temperature.

The infrared absorption spectra of all the samples are shown in Figure 2. The IR spectrum of sample 1 is well defined and resembles the spectrum obtained for a slow cooled $NiMn_2O_4$ [14]. This means that tetrahedral and octahedral bonds have formed, together with the spinel like links among them. The IR spectra of samples 2 & 3 are similar to that of nickel manganite. The frequencies of these samples, corresponding to the tetrahedral and octahedral sites alongwith their estimated bandwidths, are compared in the Table 4. The reported data corresponding to $NiMn_2O_4$ is also included in Table 4 [14] to facilitate the comparison.

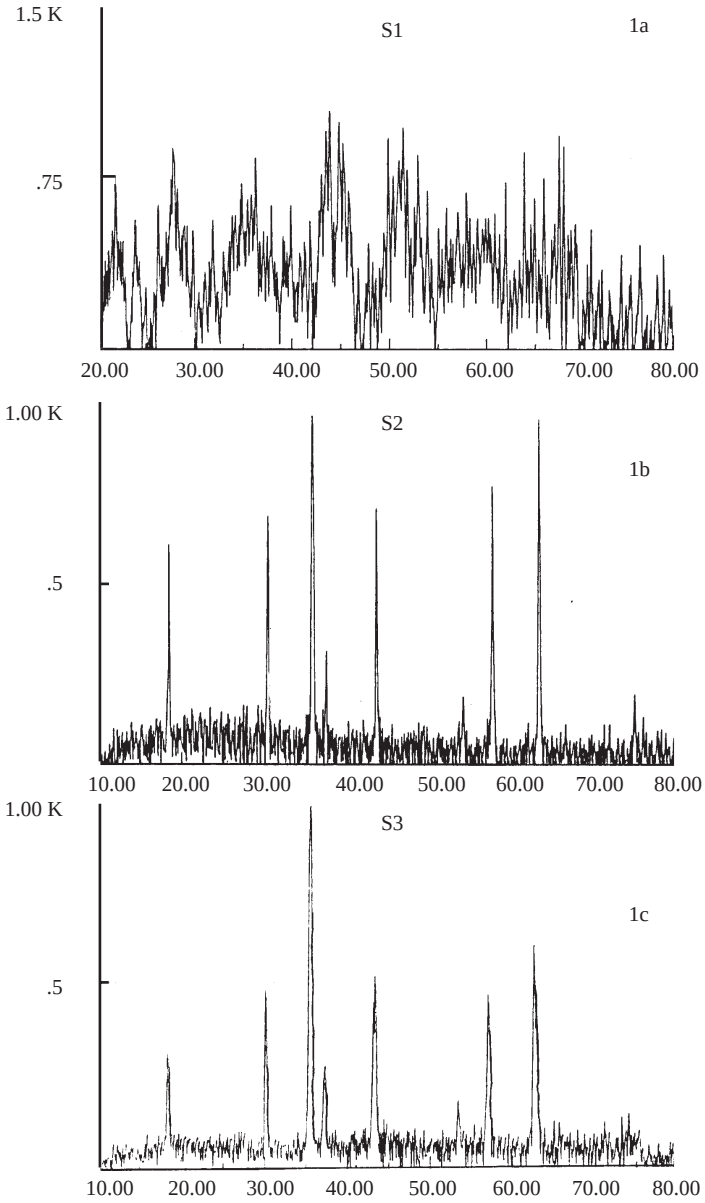

Figure 1. The XRD patterns of S1, S2, S3.

Table 1. Miller indices, Relative intensities, Interplanar distances (calculated and observed) and particle sizes of sample 2

hkl	I\I$_o$	d$_{obs}$	d$_{cal}$	Particle (size Å)
1 1 1	24	4.787	4.806	669.5
2 2 0	27	2.938	2.943	659.3
3 1 1	100	2.510	2.510	668.3
2 2 2	12	2.403	2.403	671.7
4 0 0	28	2.082	2.081	686.0
4 2 2	7	1.705	1.699	713.7
3 3 3	30	1.605	1.602	723.6
4 4 0	37	1.474	1.471	744.8
5 3 3	8	1.269	1.269	798.7

Table 2. Miller Indices, Relative Intensities, Interplanar Distances (Calculated and Observed) and Particle Sizes of Sample 3

hkl	I\I$_o$	d$_{obs}$	d$_{cal}$	Particle (size Å)
1 1 1	20	4.815	4.809	322.2
2 2 0	31	2.959	2.945	329.6
3 1 1	100	2.532	2.511	334.3
2 2 2	15	2.401	2.404	336.2
4 0 0	33	2.087	2.082	342.8
3 3 3	30	1.614	1.603	362.4
4 4 0	39	1.485	1.472	372.6

Table 3. Lattice Constants, Densities, Porosities, Average Particle Sizes and Homogenities of Samples 2 & 3

	Lattice constant (Å)	Density (gm/cc)	Porosity	Average Particle size (Å)	Inhomogenity
S2	8.325	4.490	0.2183	704.0	-0.06
S3	8.33	5.499	0.0410	342.9	-0.08

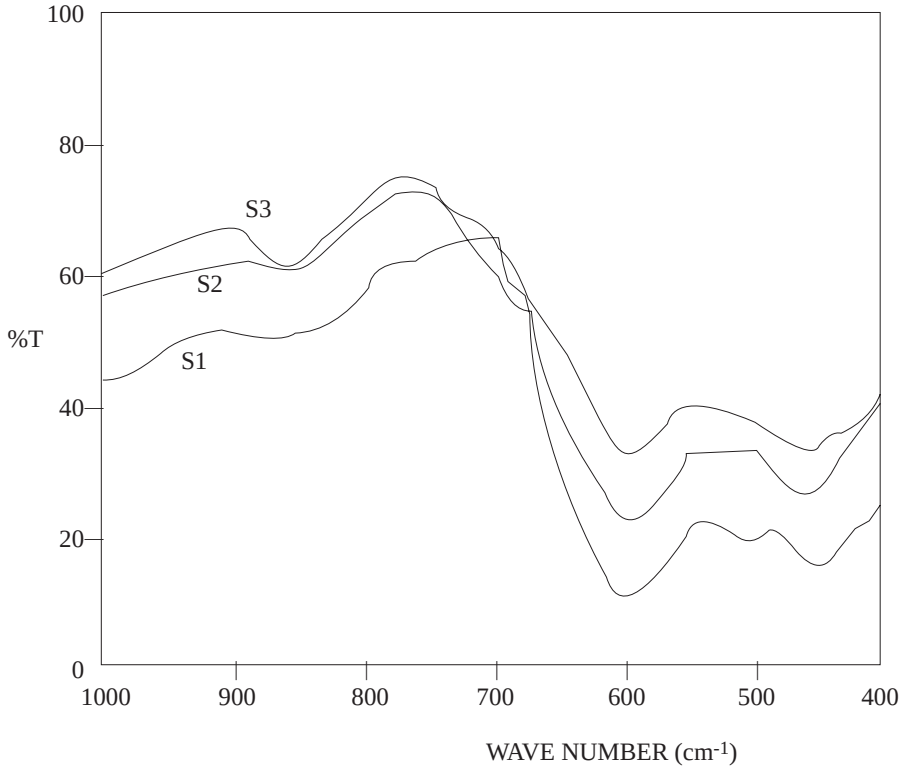

Figure 2. The IR spectras of S1, S2, S3.

Table 4. IR frequencies, Bandwidths, Types of bonds of samples S1, S2, S3 alongwith reported $NiMn_2O_4$.

Reported $NiMn_2O_4$		600 cm^{-1}/68/(T)	—	435 cm^{-1}/07/(O)
S1	856.4 cm^{-1}/—/(O)	599.9 cm^{-1}/60/(T)	507.3 cm^{-1}/—/(O)	459.1 cm^{-1}/16/(O)
S2	836.4 cm^{-1}/—/(O)	697 ck^{-1} /61/(T)	—	468 cm^{-1}/16/(O)
S3	852 cm^{-1}/—/(O)	604 cm^{-1}/64/(T)	—	476 cm^{-1}/16/(O)

(O) → Octahedral

(T) → Tetrahedral

It is interesting to note that the tetrahedral and octahedral bands of the 'lithiated' samples (S2 & S3) shift to the high energy side, with the octahedral bands shifting considerably more. As a result, the energy difference between tetrahedral and octahedral bands decrease on 'lithiation'.

The width of the tetrahedral band of the 'lithiated' samples is practically constant and equal to the reported value. On the other hand, the octahedral band appears to broaden on 'lithiation'.

IR bands corresponding to octahedral sites of both spinel and perovskite structures are in the same energy range. Therefore, on comparing the IR bands of the two structures it is concluded that the small band around 850 cm^{-1} may be due to ordered arrangement of some NiMn cations on octahedral sites. A similar band corresponding to ordered octahedral sites has been observed in perovskite [15].

For a better understanding of these observations, it is worthwhile to note the reported effects of lithiation on spinels [16-20] in which it is observed that lithium occupies vacant 16C sites in the spinel, a location which shares a face with a tetrahedral site. Therefore, lithium reduces the tetrahedral cations and transfers it to a 16C site at a temperature as high as 650 °C [16-21]. In the current investigation, since the 'lithiation' is carried out in a manner described under "experimental", and the sample is subjected to a temperature as high as 1100 °C, the contents of lithium and aluminium have been determined by plasma emission spectroscopy. The contents of lithium and aluminium are found to be 0.60 and 1.20 weight percentages of the samples. This amounts to about 4 % of 'lithiation'. This means that lithium and aluminium must have entered 16C sites of samples 2 & 3, where in Mn^{+4} to Mn^{+2} must have been reduced on octahedral site. Four cations Li^{+1}, Al^{+3}, Mn^{+2} and Ni^{+2} occupying octahedral sites resulting in greater randomisation of cation distribution on octahedral sites. The smaller masses of lithium and aluminium cations decrease the effective mass of the octahedral site. Therefore, it shifts the octahedral band to higher energy side. A small high energy shift of the tetrahedral band is indicative of weak dependance of the tetrahedral band on the octahedral band.

The d.c. electrical resistivity of sample 2 at room temperature is $7.54 \times 10^4 \Omega$ cm, which is much higher than that 54.59 Ω cm of $NiMn_2O_4$ at room temperature [7]. This may be due to $Mn^{+4} \rightarrow Mn^{+2}$ reduction in sample 2 which forbids multivalent existence of Mn cations, hence the resistivity increases. In comparison, the room temperature resistivity $5.7 \times 10^4 \Omega$ cm of sample 3 is somewhat smaller.

The plots of resistivity as a function of temperature are depicted in Figure 3 for samples 2 and 3. The activation energies of these two samples corresponding to different temperature regions are shown in Table 5. The activation energies of sample 3 are slightly smaller than those of sample 2. The different activation energies may be due to the presence of different cations on the octahedral sites.

$NiMn_2O_4$ has a break in the resistivity versus temperature plot at around 400 °C indicating a change in the cation distribution [7]. This break is not observed in samples 2 and 3, probably due to occupancy of the 16 C sites by lithium and aluminium which forbid any such change.

In conclusion, using $LiAlH_4$, a nickel manganite of moderate conductivity can be synthesized from MnO_2 at 950°C.

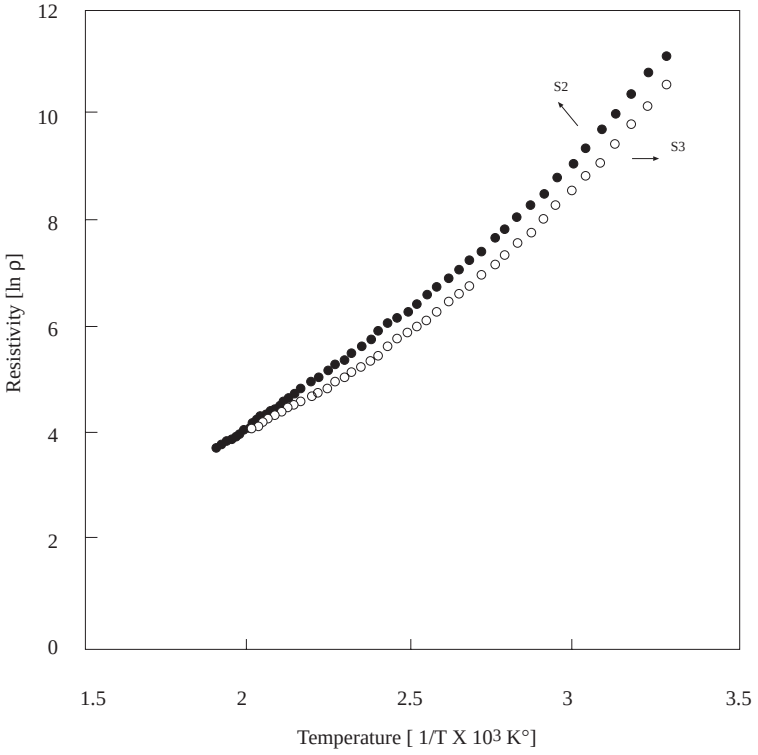

Figure 3. Plots of Resistivity v/s Temperature of S2, S3.

Table 5. Activation Energies of Samples 2 & 3

	Activation Energy	Region I	Region II	Region III
		(304-348 T°K)	(348-524T°K)	(348-524T°K)
S2	Ea in eV	0.595	0.432	0.432
		(304-329 T°K)	(329-397 T°K)	397-459 T°K)
S3	Ea in eV	0.560	0.460	0.360

References

[1] E. D. Macklen, "*Thermistors*" (Electrochemicals Publications), Ayr, Scotland, 1979.

[2] J. P. Caffin, A. Rousset, R. Carnet and A. Lagrange in "*High-Tech Ceramics*", edited by P. Vincenzini, (Elsevier, Amsterdam, 1987), **P. 1743**.

[3] E. Jabry, G. Boissier, A. Rousset, R. Carnet and A. Lagrange, *J. Physique*, **46** (1986) C1843.

[4] R. Legros, R. Metz, J. P. Caffin, A. Lagrange and A. Rousset in *"Better Ceramics Through Chemistry III"*, edited by C. J. Brinker et al (Elsevier, New York, **121** (1988) P. 251.

[5] R. Metz, J. P. Caffin, R. Legros and A. Rousset,*J. Mat. Sci.*, **24** (1989) 83.

[6] A. O. B. Sinha, N. R. Sanjana and A. B. Biswas, *Acta. Cryst.*, **10** (1957) 439.

[7] V. A. M. Brabers and J. C. J. M. Terhell, *Phy. Stat. Sol(a)*, **69** (1982) 325.

[8] P. K. Baltzer and J. G. White, *J. Appl. Phys.*, **29** (1958) 445.

[9] L. V. Azaroff and Z. Kristallogr, **112** (1959) 33.

[10] F. A. Cotton and G. Wilkinson, Advanced Inorganic Chemistry [Publisher and Wiley Eastern Limited, P. 837].

[11] i) Russed, *J. Am. Ceram. Soc.*, **18** (1935) 1. ii) H. Looyenga, *Physica A*, **31** (1965) 401.

[12] P. Scherrer, *Cottin Nachricht*, **2** (1918) 98.

[13] Kawashima, *J. Am. Ceram. Soc.*, **6**, 66 (1983) 421.

[14] V. A. M. Brabers, *Phys. Stat. Sol(a)*, **12** (1972) 629.

[15] N. G. Durge, Doctoral Thesis, *Univ. of Bombay*, (1996).

[16] M. N. Tackeray, W. I. F. David and S. B. Goodenough, *Mat. Res. Bull.*, **17** (1982) 785.

[17] M. S. Islam and R. A. Catlow, *J. Sol. State Chem.*, **77** (1988) 180.

[18] L. A. de Picciotto & M. N. Thackeray, *Mat. Res. Bull*, **2** (1986) 583.

[19] M. N. Thackeray, W. I. F. David, P. G. Bruce and J. B. Goodenough, *Mat. Res. Bull.*, **18** (1983) 461.

[20] C. J. Chen, M. Greenblatt, *Solid. State Ionics*, **18 & 19** (1986) 838.

[21] C. J. Chen, M. Greenblatt, *Mat. Res. Bull.*, **21** (1986) 609.